Temporal context calibrates interval timing

[1,2]Mehrdad Jazayeri & [2]Michael N. Shadlen

[1]*Helen Hay Whitney Foundation*

[2]*HHMI, NPRC, Department of Physiology and Biophysics, University of Washington, Seattle, Washington*

Supplementary Information

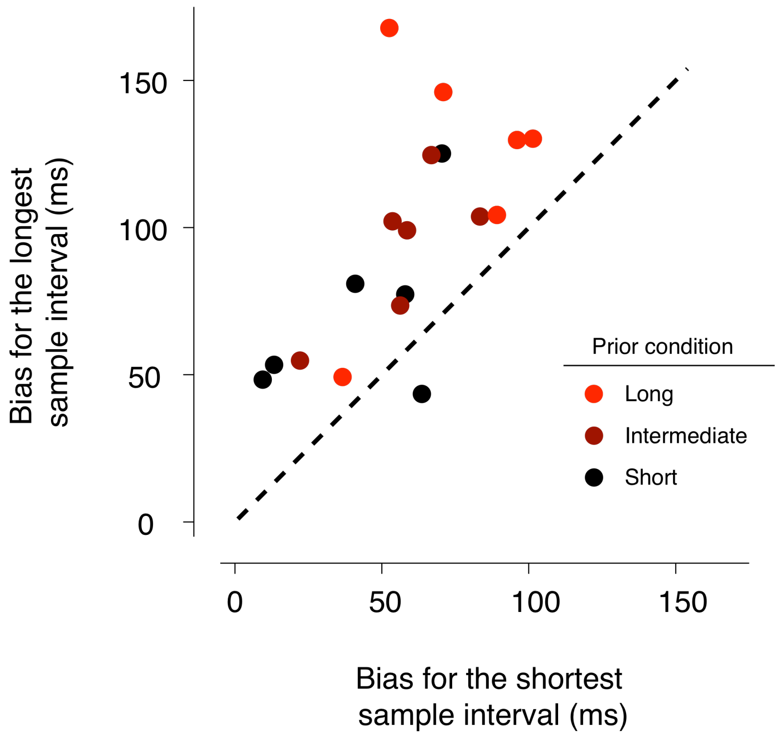

Figure S1. Magnitude of the bias for short and long sample intervals. For each prior condition and each subject, the magnitude (i.e. absolute value) of the bias associated with the longest sample interval is plotted against the magnitude of the bias associated with the shortest sample interval. Across subjects and prior conditions, the magnitude of the bias was significantly larger for the longest sample interval compared to the shortest sample interval (Wilcoxon signed-rank test; $p<0.001$). This result is consistent with the observation that going from "Short" to "Intermediate" to "Long" prior conditions, the overall bias increased in magnitude (**Fig. 2**, main text). Black, dark red, and light red show the "Short", "Intermediate", and "Long" prior conditions respectively.

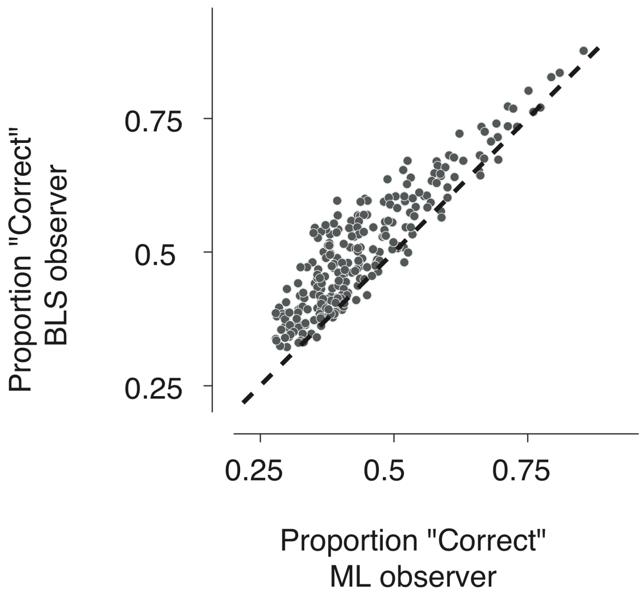

Figure S2. Performance of the Bayes-least-squares (BLS) and the maximum likelihood (ML) estimators in the time reproduction task. We simulated the behavior of BLS and ML observers in the time reproduction task consisting of 1000 trials in which the sample intervals were drawn from a discrete uniform prior distribution with 11 values ranging between 671 and 1023 ms (the "Intermediate" prior condition in the main experiment). For each observer model, we repeated the simulation while varying the measurement and production Weber fractions independently between 0.05 and 0.2 in steps of 0.01. Each dot in the plot corresponds to a particular pair of measurement and production Weber fractions. Production times within 10% of the sample intervals were considered "correct". The scatter plot shows the proportion "correct" for the BLS observer versus the ML observer. The BLS observer, whose production times were biased towards the mean of the prior (**Figure 5g**, main text), consistently outperformed the ML observer.

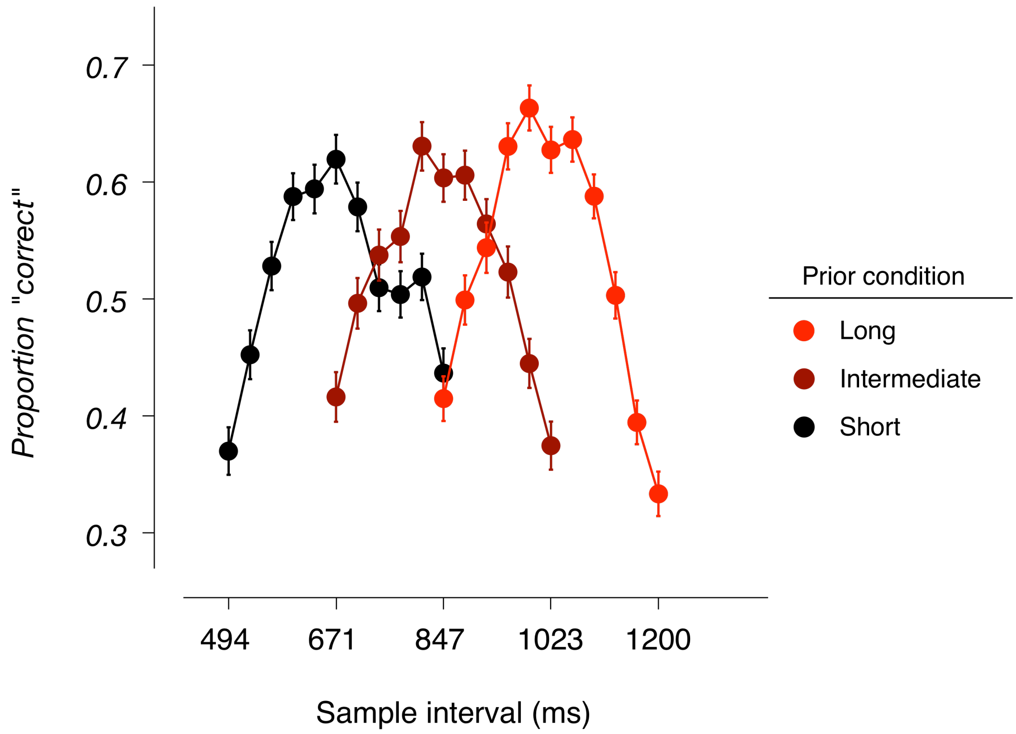

Figure S3. Positively reinforced trials for each prior condition. For each prior condition, the mean (solid dots), and standard error (error bars) of the proportion of trials positively reinforced ("correct") across subjects is plotted against the sample interval. The overall range of the proportion of "correct" trials goes from ~0.35 to ~0.65. For each prior condition, the maximum (minimum) number of "correct" trials corresponded to the intermediate (extreme) sample intervals. Black, dark red, and light red show the "Short", "Intermediate", and "Long" prior conditions respectively.

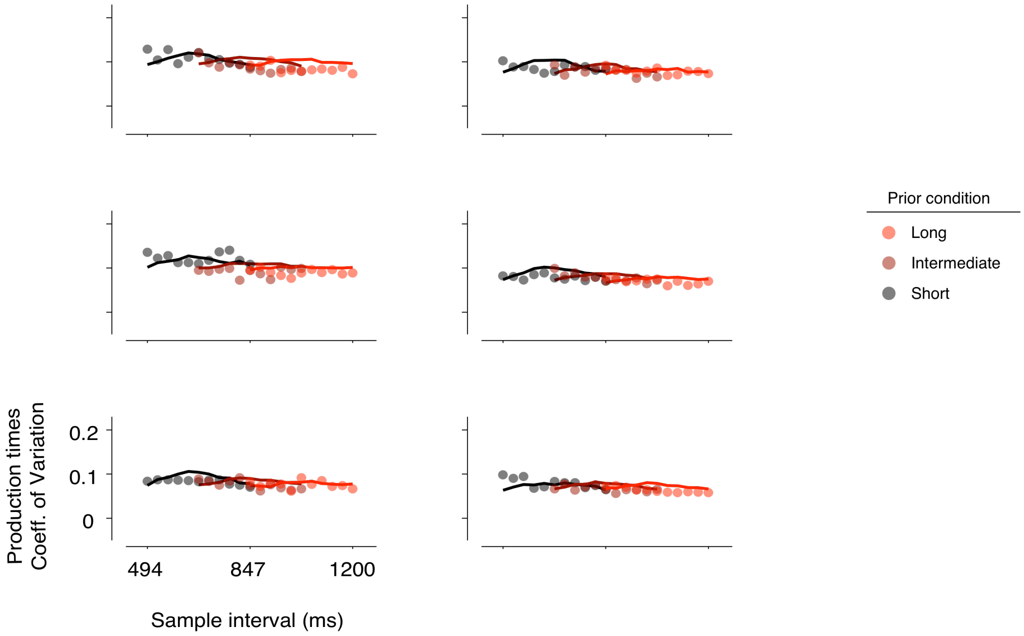

Figure S4. Coefficient of variation (CV) of production times. The 6 panels show the CV (ratio of the standard deviation to the mean) of production times for the 6 subjects as a function of sample interval sorted by the prior condition. The filled circles are CV values computed from the subjects' production times, and the solid lines are the CV values computed from simulations of the best-fitted Bayes least squares (BLS) model. Black, dark red, and light red show the "Short", "Intermediate", and "Long" prior conditions respectively.

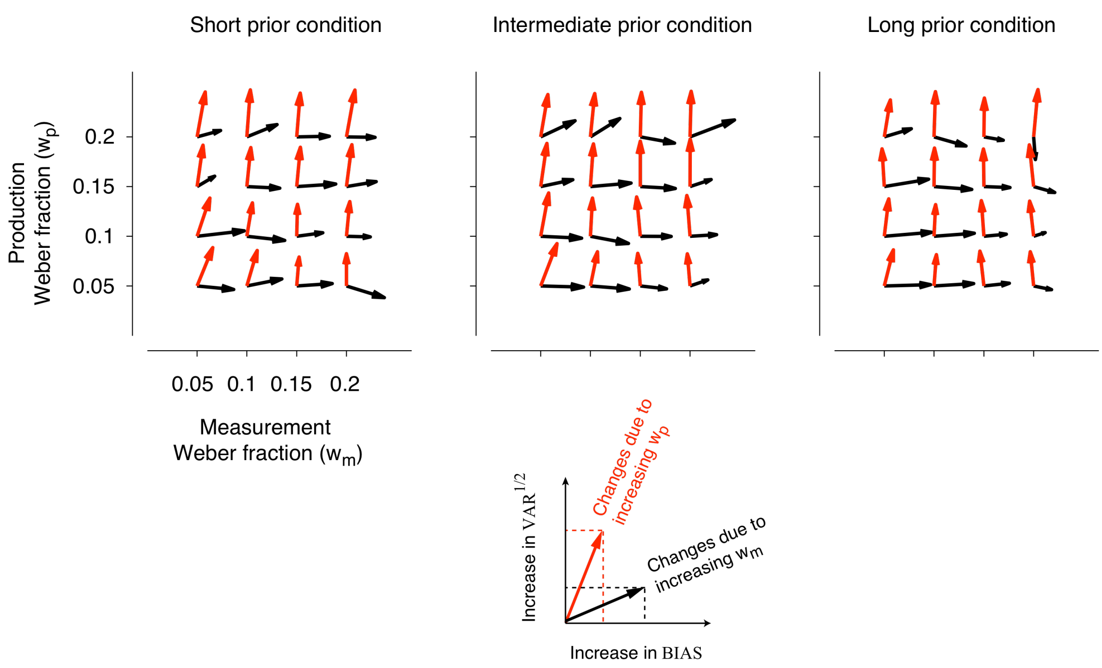

Figure S5. Changes in BIAS and VAR with respect to the measurement and production noise. In the three top panels, arrows show the gradient of the overall bias (BIAS), and variability ($VAR^{1/2}$) of production times (as defined in the main text) for the BLS observer model with respect to the measurement and production Weber fractions (w_m and w_p respectively) for the three prior conditions. The origin of each arrow corresponds to the w_m and w_p values at which the gradient was computed, and its horizontal/vertical components reflect changes in BIAS and $VAR^{1/2}$ respectively (lower panel). Gradients with respect to w_m (black arrows) have a strong horizontal component indicating that w_m mainly controls the BIAS. In contrast, gradients with respect to w_p (red arrows) are mostly vertical indicating that w_p mainly controls the $VAR^{1/2}$. In other words, w_m and w_p are both important parameters in the model as they capture distinct statistics of production times.

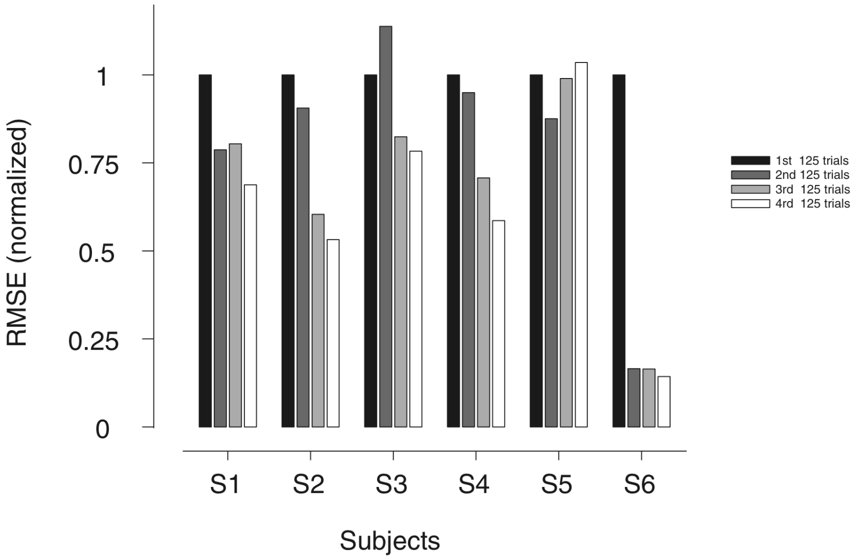

Figure S6. Improvement of performance during the learning stage. The plot shows the improvement in performance by computing the overall root mean square error (RMSE) of production times from data collected during the training session preceding the first test session. The plot shows the RMSE in the first 500 trials (learning stage), sorted into four bins each containing 125 trials. For each subject, RMSE values were normalized to RMSE value in the first bin. The graph shows a consistent improvement of performance (reduction in RMSE) over these 500 trials across subjects. For one of the subjects (S6), the improvement was clear after the 1st 125 trials.

			S1	S2	S3	S4	S5	S6
BLS 1	Measurement std Weber Production std Weber	**AIC**	10087	10282	12226	8768	10226	8197
		w_m	0.0935	0.1028	0.1436	0.1208	0.1053	0.0481
		w_p	0.0858	0.0635	0.0894	0.0583	0.0623	0.0625
BLS 2	Measurement std Weber Production std fixed	**AIC**	10178	10362	12252	8774	10309	8142
		w_m	0.1019	0.1030	0.1431	0.1229	0.1047	0.0519
		σ_p (ms)	69.60	54.64	75.92	47.66	50.11	49.31
BLS 3	Measurement std fixed Production std Weber	**AIC**	14505	18532	18647	15320	16530	15510
		σ_m (ms)	69.45	77.26	80.53	70.29	64.59	69.01
		w_p	0.1563	0.2060	0.1923	0.1793	0.1607	0.1866

Table S1. Model comparison: BLS models with different forms of measurement and production noise. In the original model (BLS1), the standard deviation (std) of both measurement and production noise was proportional to the base interval (constant Weber fraction). The three data rows associated with BLS1 show the Akaike Information Criterion (AIC), measurement Weber fraction (w_m), and production Weber fraction (w_p), respectively, for the six subjects (S1 to S6). In the BLS2 model, the measurement noise was associated with a constant Weber fraction (w_m), but the production noise was Gaussian with a fixed standard deviation (σ_p). The BLS3 model was the reverse with a constant Weber fraction for production (w_p), and a fixed standard deviation (σ_m) for the measurement. For each subject, the model with the smallest AIC is underlined. The quality of fits for BLS1 and BLS2 were comparable although BLS1 was superior for 5 out of 6 subjects. BLS2 failed to capture the larger production time variance associated with longer sample intervals (**Fig. S5**). BLS3 was markedly inferior to both BLS1 and BLS2 models as it failed to capture the characteristic increase in bias associated with longer sample intervals (**Fig. 5b,S1**). Note that all models have two free parameters.

	Measurement noise model	Production noise model
BLS 1	$p(t_m \mid t_s) = \frac{1}{\sqrt{2\pi(w_m t_s)^2}} e^{\frac{-(t_s - t_m)^2}{2(w_m t_s)^2}}$	$p(t_p \mid t_e) = \frac{1}{\sqrt{2\pi(w_p t_e)^2}} e^{\frac{-(t_p - t_e)^2}{2(w_p t_e)^2}}$
BLS 2	$p(t_m \mid t_s) = \frac{1}{\sqrt{2\pi(w_m t_s)^2}} e^{\frac{-(t_s - t_m)^2}{2(w_m t_s)^2}}$	$p(t_p \mid t_e) = \frac{1}{\sqrt{2\pi\sigma_p^2}} e^{\frac{-(t_p - t_e)^2}{2\sigma_p^2}}$
BLS 3	$p(t_m \mid t_s) = \frac{1}{\sqrt{2\pi\sigma_m^2}} e^{\frac{-(t_s - t_m)^2}{2\sigma_m^2}}$	$p(t_p \mid t_e) = \frac{1}{\sqrt{2\pi(w_p t_e)^2}} e^{\frac{-(t_p - t_e)^2}{2(w_p t_e)^2}}$

Table S2. BLS models with different forms of measurement and production noise. Parameters are defined in the caption of **Table S1** and the Methods section of the main manuscript.